Macromolecular Materials and Engineering
www.mme-journal.de

Electroactive Silk Fibroin Films for Electrochemically Enhanced Delivery of Drugs

*Seyed T. Mousavi, Garry R. Harper, Sofia Municoy, Mark D. Ashton, David Townsend, Ghazi H. K. Alsharif, Vasileios K. Oikonomou, Melike Firlak, Sophie Au-Yong, Bethany E. Murdock, Geoffrey R. Akien, Nathan R. Halcovitch, Sara J. Baldock, Mohamad Fazilati, Oleg V. Kolosov, Benjamin J. Robinson, Martin F. Desimone, and John G. Hardy**

Biomaterials capable of controlling the delivery of drugs have the potential to treat a variety of conditions. Herein, the preparation of electrically conductive silk fibroin film-based drug delivery devices is described. Casting aqueous solutions of *Bombyx mori* silk fibroin, followed by drying and annealing to impart β-sheets to the silk fibroin, assure that the materials are stable for further processing in water; and the silk fibroin films are rendered conductive by generating an interpenetrating network of a copolymer of pyrrole and 3-amino-4-hydroxybenzenesulfonic acid in the silk fibroin matrix (characterized by a variety of techniques including circular dichroism, Fourier-transform infrared spectroscopy, nuclear magnetic resonance, Raman spectroscopy, resistance measurements, scanning electron microscopy-energy dispersive X-ray spectroscopy, thermogravimetric analysis, X-ray diffraction, and X-ray photoelectron spectroscopy). Fibroblasts adhere on the surface of the biomaterials (viability assessed using an (3-(4,5-dimethylthiazol-2-yl)-2,5-diphenyltetrazolium bromide) assay and visualized using a confocal microscope), and a fluorescently labeled drug (Texas-Red Gentamicin) can be loaded electrochemically and released (μg cm^{-2} quantities) in response to the application of an electrical stimulus.

Natural[1–4] and recombinant[5,6] silk proteins are popular components of biomaterials for drug delivery, tissue engineering, and regenerative medicine, owing to their processability, biocompatibility, and biodegradability, demonstrating their promise in various biomedical niches in vitro, and in preclinical trials.[7] Silk-based biomaterials in a selection of materials morphologies (including films, fibers, films, and hydrogels) have been prepared using the silk proteins produced by various species (silkworms, spiders, etc.)[8] and recombinantly,[5,6] as have composites including such proteins.[9,10]

The development of instructive biomaterials capable of the imparting signals to tissues in which they are in contact with is an inherently interdisciplinary research field, and the subject of increasing attention from researchers in academia and industry.[11–13] Silk-based materials with specific chemical,

S. T. Mousavi, Dr. G. R. Harper, M. D. Ashton, Dr. D. Townsend, V. K. Oikonomou, Dr. M. Firlak, S. Au-Yong, B. E. Murdock, Dr. G. R. Akien, Dr. N. R. Halcovitch, Dr. S. J. Baldock, Dr. J. G. Hardy
Department of Chemistry
Lancaster University
Lancaster LA1 4YB, UK
E-mail: j.g.hardy@lancaster.ac.uk

S. T. Mousavi, Prof. M. Fazilati
Department of Biochemistry
Payame Noor University
P. O. Box 19395-3697, Isfahan 81581-84431, Iran

Dr. S. Municoy, Prof. M. F. Desimone
Universidad de Buenos Aires, Consejo Nacional de Investigaciones Científicas y Técnicas (CONICET)
Instituto de Química y Metabolismo del Fármaco (IQUIMEFA)
Facultad de Farmacia y Bioquímica, Junín 956
Piso 3° (1113), Buenos Aires 1113, Argentina

The ORCID identification number(s) for the author(s) of this article can be found under https://doi.org/10.1002/mame.202000130.

G. H. K. Alsharif, S. Au-Yong, Prof. O. V. Kolosov, Dr. B. J. Robinson
Department of Physics
Lancaster University
Lancaster LA1 4YW, UK

G. H. K. Alsharif
Physics Department, Faculty of Science
Taibah University
Tayba, Medina 42353, Saudi Arabia

Dr. M. Firlak
Department of Chemistry
Gebze Technical University
Gebze, Kocaeli 41400, Turkey

Dr. B. J. Robinson, Dr. J. G. Hardy
Materials Science Institute
Lancaster University
Lancaster LA1 4YB, UK

DOI: 10.1002/mame.202000130

mechanical, and topographical cues have enabled important properties to be engineered into materials for patient-specific personalized medical devices.[14] Indeed, it is possible to prepare silk-based materials with biodegradation rates and mechanical properties controlled by their processing conditions (e.g., choice of solvents, temperatures, etc.), the type of silk used (natural/recombinant), or their modification by chemical or biochemical means.[15] Preclinical studies using silk-based biomaterials are promising for a variety of applications and tissue niches.[16]

For many biomedical applications in vitro, ex vivo and in vivo, the ability to deliver active ingredients in a controlled fashion is very appealing, and many stimuli have been investigated to achieve this (e.g., ionic strength, light, magnetic fields, pH, ultrasound, etc.),[12,17–20] and a variety of stimuli-responsive silk-based materials have been reported.[21–28]

Electrical stimuli offer potential for precise control of medical devices, in part because of their ability to control the magnitude of currents/voltages and duration of pulses/intervals. Conducting biomaterials based on organic electronic materials (OEMs) including derivatives of carbon nanotubes, graphene, and conducting polymers have potential for a variety of biomedical applications for long term use (e.g., electrodes to record/stimulate cellular activity) or short term use (e.g., drug delivery and tissue engineering).[29,30] Conductive silk-based materials have been successfully used for biomedical applications, including as electrodes for recording endogenous signals, or indeed as tissue scaffolds.[21,25,26,31–42] The use of electricity for drug delivery is exciting,[43–47] and has been clinically translated for certain specific applications (e.g., electroporation/iontophoresis).

Here, we describe the results of our investigation of conductive films (**Figure 1**A) based on an interpenetrating network of *Bombyx mori* silkworm silk fibroin and conducting polymers (a copolymer containing pyrrole and an aniline derivative, the synthesis of which is depicted in Figure 1B).[35] The films were characterized by a variety of techniques (including circular dichroism (CD), Fourier-transform infrared spectroscopy (FTIR), nuclear magnetic resonance (NMR), Raman spectroscopy, resistance measurements, scanning electron microscopy-energy dispersive X-ray spectroscopy (SEM-EDX), thermogravimetric analysis (TGA), X-ray diffraction (XRD), and X-ray photoelectron spectroscopy (XPS)), as was the adhesion of fibroblasts to the films, and their ability to deliver a fluorescently labeled clinically relevant drug (Texas-Red Gentamicin) in vitro.

B. mori silk fibroin was degummed, dissolved (in a solution of $CaCl_2$, ethanol, and water), dialyzed against water and subsequently cast in petri dishes, yielding films had thicknesses of ≈100 μm that are hereafter referred to as "as cast." The as cast films were subsequently immersed in methanol and are hereafter referred to as "methanol treated." The films were rendered conductive by generation of an interpenetrating network of a self-doped conducting polymer within the silk fibroin matrix (Figure 1A,B) by adaptation of the literature.[35] The self-doped conducting polymers were composed of pyrrole and 3-amino-4-hydroxybenzenesulfonic acid and their polymerization within the silk fibroin films was initiated by ammonium persulfate and ferric chloride (Figure 1B),[35] followed by thoroughly washing with water and ethanol to remove low molecular weight components that were not entrapped within or attached to the silk fibroin matrix (e.g., initiators, monomers, oligomers, and polymers), such films are subsequently referred to as "conductive" films, the sheet resistance of which were 26.8 ± 1.3 MΩ □ as measured using a nanoprober (Figure S1, Supporting Information).

SEM (Figure 1C–E) showed that the surface of the as cast films are relatively smooth on the μm scale, whereas the

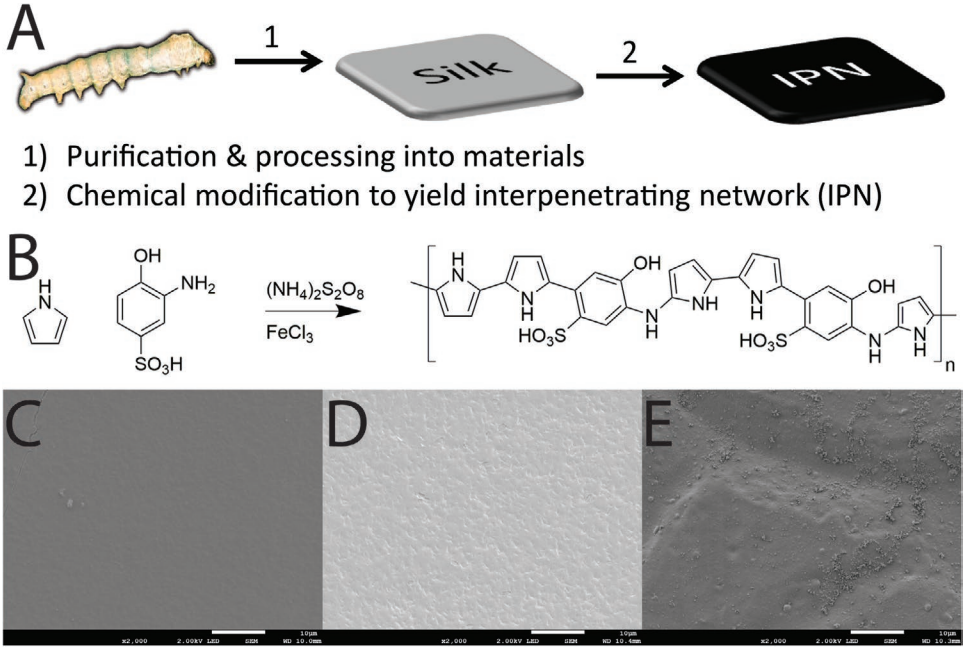

Figure 1. A) Purification and processing of silk fibroin to generate materials (films) and subsequently generate a conductive interpenetrating network (IPN). B) Schematic of the synthesis of the conducting polymer (with a random sequence of monomers) utilized in the IPNs studied. SEM images of the films: C) as cast films, D) methanol treated films, and E) conductive films. Scale bars (white) represent 10 μm.

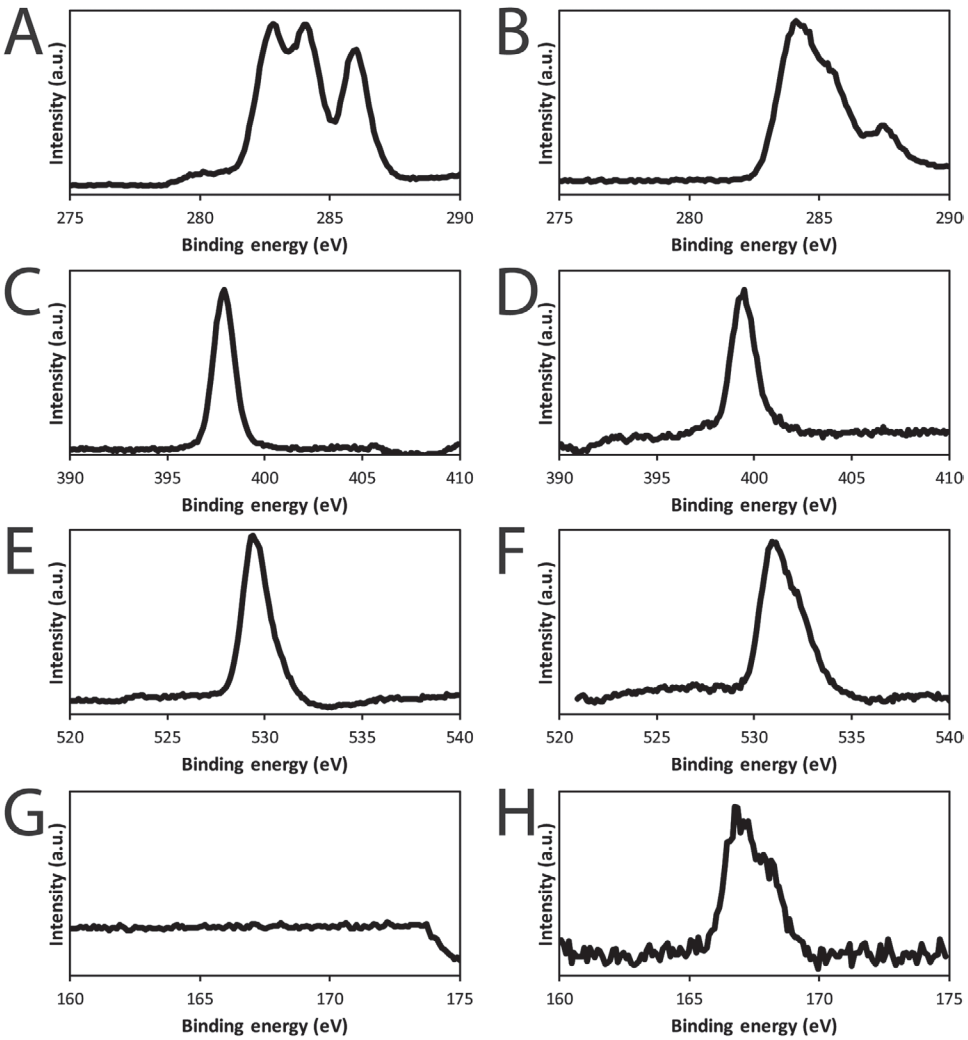

Figure 2. XPS data. Methanol treated films: A) C 1s, C) N 1s, E) O 1s, and G) S 2p. Conductive films: B) C 1s, D) N 1s, F) O 1s, and H) S 2p.

methanol treated films are somewhat rougher due to reorganization of the polymer chains within the matrix during β-sheet formation, and the conductive films have aggregates of conducting polymers (composed of nanoparticles typically of 50–500 nm; Figure S2, Supporting Information) on their surface, results which are in line with the literature.[35] EDX analysis (Figure S3, Supporting Information) showed elemental signals characteristic of Au (instrumental background, M 2.123 keV), Si (glass substrate, Kα 1.739 keV), and the elements associated with the silk fibroin-based materials for as cast and methanol treated films: C (Kα 0.277 keV), N (Kα 0.392 keV), O (Kα 0.525 keV), and S (Kα 2.307 keV). Peaks for Ca (Kα 3.690 keV) and Cl (Kα 2.621 keV) residual from their initial processing, but absent in the spectra of the conductive films owing to their extensive washing, and the conductive films also showed stronger peaks for S owing to its presence on the aniline derivative incorporated in the backbone of the conducting polymer. XPS spectra of the methanol treated and conductive films (**Figure 2**; Figure S4, Supporting Information) confirm that the surface chemistry of the films has changed, with changes in the appearance of all the C 1s, N 1s, O 1s, and S 2p spectra of the films after rendering them conductive due to the new species present in the backbone of the conducting polymers. The combination of SEM, EDX, and XPS data demonstrate the successful modification of the surface of the films with conducting polymers.

XRD data (Figure S5, Supporting Information) suggested the as cast films were largely amorphous, confirmed by the peak at $2\theta \approx 20°$, whereas the methanol treated films were somewhat more crystalline with peaks at $2\theta = 19.9°$ and 24.0° suggesting β-sheet content;[35,48] and the XRD data for the conductive films was not significantly different from the methanol treated films. TGA revealed that the films contained residual water and that the methanol treated and conductive films were stable in excess of 200 °C, with a slightly earlier onset of degradation for the conductive films (Figure S6, Supporting Information).[49] The thermal stability of the materials up to 200 °C offers potential for sterilization by steam in an autoclave at 121 °C for 20 min, or dry sterilization in an autoclave at 170 °C for 60 min, albeit with potential consequences for the mechanical/electrical properties of the materials,[50] and an optimal method of sterilization will be dependent upon the specific application, and thermal stability of any drugs/active ingredients incorporated.

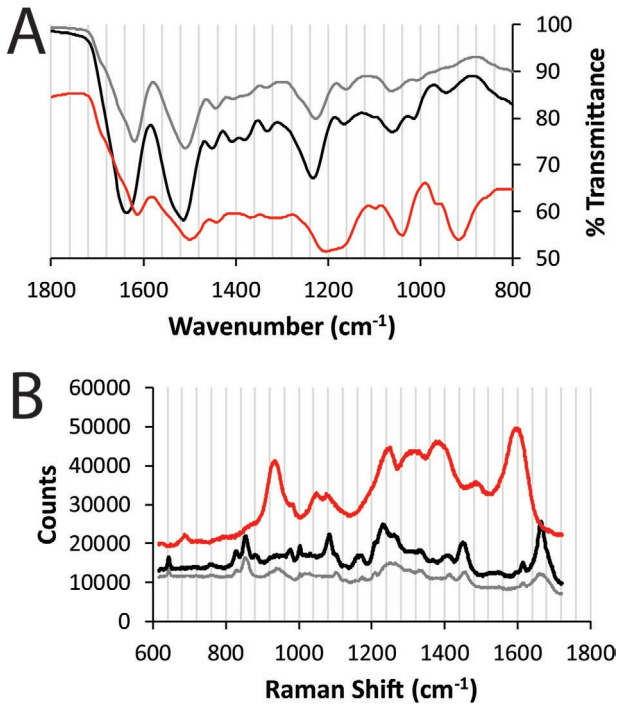

Figure 3. A) FTIR spectra of "as cast" (gray), methanol treated (black), and conductive (red) films. B) Raman spectra of "as cast" (gray), methanol treated (black), and conductive (red) films.

Infrared spectra (**Figure 3**A) for the as cast films exhibit peaks in the amide I region at 1605–1615 cm^{-1} characteristic of aggregated strands, and a shoulder at 1616–1621 cm^{-1} characteristic of aggregated beta strands, and the amide II region at 1510 cm^{-1} characteristic of turns and unhydrated peptide groups.[51] The methanol treated films exhibit a strong peak between 1621 and 1637 cm^{-1} in the amide I region and a peak at 1520 cm^{-1} in the amide II region characteristic of β-sheets (and a shoulder at 1540 cm^{-1} characteristic of α-helical content).[52] The conductive films displayed significant shoulders at 1541 and 1499 cm^{-1} are characteristic of oligoanilines and an increase in α-helical content relative to β-sheets, the peaks evident at 1204 cm^{-1} (asymmetric S=O stretching), 1037 cm^{-1} (C–H in-plane deformation and/or symmetric S=O stretching), 917 cm^{-1}, and a shoulder at 895 cm^{-1} (C–H out-of-plane deformation of aromatic rings and/or bipolaron bands)[35] confirm that the conductivity of the films is due to the presence of the polymers depicted in Figure 1.

FDA approved poly(ethylene glycol)s (PEGs) are widely used for concentrating protein solutions by dialysis and FTIR spectra of the as casts films showed some evidence of traces of PEGs that transferred across the dialysis membrane from the presence of a small peak in spectra between 1150–1085 cm^{-1}, which could be attributable to ether bonds in PEGs. However it is noteworthy that this overlaps with the primary OH moieties displayed on the serine residues displayed on the backbone of the silk fibroin (1150–1085 cm^{-1}, ≈9.5% of the residues in the backbone of *B. mori* silk fibroin), and the secondary OH moieties displayed on the threonine residues displayed on the backbone of the silk fibroin (1124–1087 cm^{-1}, ≈2% of the residues in the backbone of *B. mori* silk fibroin). There is a shift in the shape of this peak after treatment of the films with methanol indicative of the methanol dissolving traces of PEG in the films, and the small peak that remains is due to serine and threonine instead of PEG.

CD data (Figures S7–S9 and Table S1, Supporting Information) confirms the presence of α-helical and β-sheet content in all films. Interestingly, the chemical modification process to render the films conductive altered the balance of secondary structural elements in the films (the conductive films had an increase in α-helical content relative to β-sheet content in line with the FTIR data) which potentially accounts for earlier onset of thermal degradation for the conductive materials observed in the TGA data (Figure S6, Supporting Information).

Raman spectra (Figure 3B) for the as cast films exhibited amide I peaks at 1657 cm^{-1} characteristic of silk I, random coil conformation or α-helices (a small peak at 1669 cm^{-1} potentially due to some β-sheets), the peak at 1616 cm^{-1} is attributed to phenylalanine, tyrosine and trypophan,[53–57] and the amide III range has maxima at 1272, 1255, and 1249 cm^{-1}, which is characteristic of silk fibroin with a prevailing random-coil conformation, in line with the literature.[56] The methanol treated films exhibited a strong amide I peak at 1667 cm^{-1} characteristic of β-sheets, and there is a strong amide III peak at 1230 cm^{-1} characteristic of β-sheets, indicating the film has a higher β-sheet content after methanol treatment in line with the FTIR and XRD data, and literature.[52,56] The conductive films exhibited more complex spectra owing to the variety of species present which overlap the peaks from the silk fibroin. The peaks were assigned in accordance with the literature as follows: 656 cm^{-1} (sulfate), 686 cm^{-1} (C–H wagging), 934 cm^{-1} (C–C ring deformation, bipolarons), 1050 cm^{-1} (C–H in-plane deformation, polarons), 1079 cm^{-1} (C–H in-plane deformation, bipolarons), 1242 cm^{-1} (antisymmetric C–H in-plane bending, ring stretching), 1329 cm^{-1} (C–C in-ring, antisymmetric C–N stretching), 1385 cm^{-1} (C–C in-ring, antisymmetric C–N stretching, C–H bending, N–H bending stretching), 1490 cm^{-1} (C=N stretching in quinonoids), 1496 cm^{-1} (C–C, C=N stretching), 1512 cm^{-1} (N–H bending), 1599 cm^{-1} (C=C in-ring, C–C inter-ring stretching), and 1623 cm^{-1} (C-C stretching of the benzenoid ring vibrations).[58,59] The Raman spectra also confirms that the conductivity of the films is due to the presence of the polymers depicted in Figure 1.

The solid state cross polarized magic angle spinning (CP-MAS) ^{13}C NMR spectra of the as cast films (Figure S10, Supporting Information), methanol treated films (Figure S11, Supporting Information), and conductive films (Figure S12, Supporting Information) show structural transitions upon methanol treatment and chemical modification. The CP-MAS spectra for the as cast and methanol treated films are assigned in accordance with the chemical shifts reported in the literature.[60] Ala Cβ at 16.5 ppm for distorted β-turn and/or random coil, or 19.6 ppm for the β-sheet peak A, and 21.7 ppm for the β-sheet peak B (β-sheet peaks A and B arise from differences in the intermolecular structure arrangement.[60] Tyr Cβ at 36.1 ppm for random coils, and 40.3 ppm peak for β-sheets. Gly Cα peak at 42.6 ppm; Ala Cα peak at 50 ppm; Ser Cα peak at 55 ppm; Ser Cβ peak at 61.5 ppm for random coils, and peaks at 64.0 and 65.5 ppm for β-sheet A and β-sheet B, respectively. Gly CO peak at 165 ppm, Ala/Ser CO peak at 170 ppm for

β-sheets, and Ala CO peak at 175 ppm for random coils. The chemical modification step introduced a number of new peaks at: 116.5 ppm (Cα–Hα), 128 ppm (Cβ–Hβ) in Py units, and 117 ppm (Cε–Hε), and 123 ppm (Cγ–Hγ), respectively.[61] There is a small peak at ≈70 ppm which could be due to CH_2O in traces of PEG in the films, however, this is more likely to be attributed to the β-carbon in threonine residues as the integral is similar for each film (as cast, methanol treated and conductive), and traces of PEG are below the limit of detection of the NMR.

Analogously modified *B. mori* silk fibroin foams were capable of electrical stimulation of human mesenchymal stem cells, and cytocompatible over a period of 30 days [Kaplan-mbs], and to confirm these materials were also cytocompatible, fibroblasts were cultured on them and cell viability was evaluated by (3-(4,5-dimethylthiazol-2-yl)-2,5-diphenyltetrazolium bromide) (MTT) assay[62] (**Figure 4**A). We observed similar proliferation for the cells grown on the control tissue culture plastic as for cells cultured on both nonconductive and conductive silk fibroin materials for the first three days, which continued over a period of a week, albeit more slowly on the silk fibroin-based materials. The positive cell adhesion and proliferation were confirmed by fluorescence microscopy (Figure 4B).[63,64]

The development of stimuli-responsive drug delivery systems offers a variety of potentially exciting applications, where the control of the delivery offers opportunities to control the chronopharmacology of the drug in line with the chronobiology of the condition to be treated, and a variety of drugs have been delivered from conducting polymer-based materials.[45,65,66] The conductive films were doped/loaded with drugs electrochemically from aqueous solutions of the drugs. We attempted to release dexamethasone phosphate from the films, however its release was below the limit of detection of UV–visible spectroscopy. Consequently, we electrochemically loaded 1 μg of Texas-Red Gentamicin and subsequently studied its release using fluorescence spectroscopy due to its increased sensitivity and lower limit of detection. We observed low levels of passive release of Texas-Red Gentamicin from the films and markedly enhanced delivery upon the application of an electrical stimulus over the course of the experiments (Figure 4C). The delivery of antibiotics is important for a variety of applications, particularly for invasive surgical procedures where the costs associated with treating infections arising from surgeries (potentially including subsequent surgical procedures to remove/replace the implant) are significant. The ability to control the delivery of antibiotics in an on/off fashion offers an opportunity to tune the delivery profile of the antibiotic in a patient specific manner.

In conclusion, the characterization by CD, FTIR, NMR, Raman spectroscopy, resistance measurements, SEM-EDX, TGA, XRD, and XPS together confirm the successful preparation of *B. mori* silk fibroin films and their subsequent modification to yield a conductive interpenetrating network of polymers. The methodology reported should be translatable to other silks (of natural or recombinant sources),[5,67–69] silk-inspired polymers and proteins,[70] and a multitude of other polymer-based materials thereby facilitating their use for various bioelectronics applications. The fluorescently labeled antibiotic released here is an excellent model for other drugs that can potentially be released from such materials.

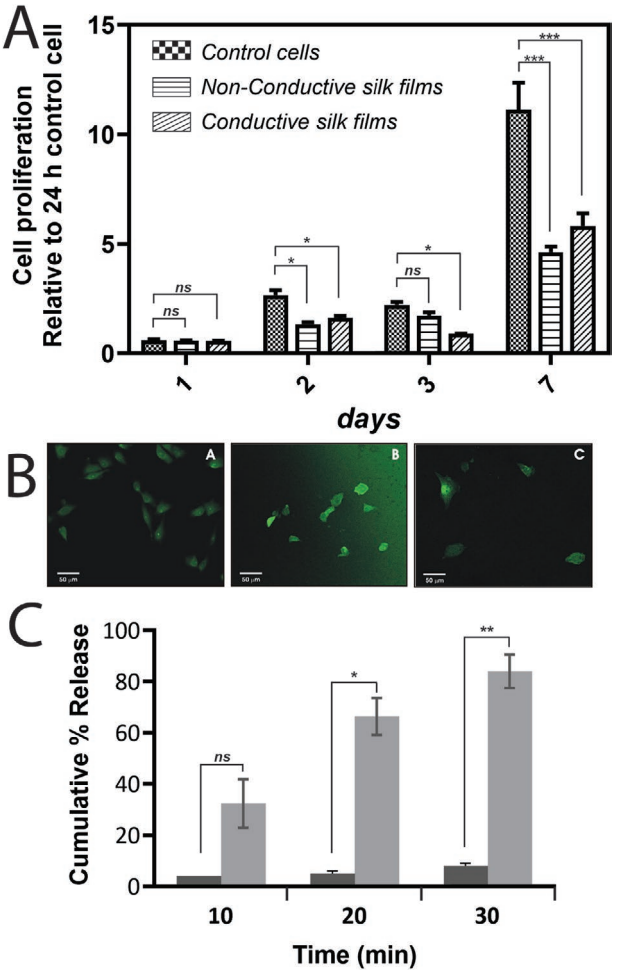

Figure 4. A) Proliferation of 3T3 fibroblast cells as measured by the MTT test after exposure to nonconductive and conductive silk fibroin films. Results are expressed as mean ± SD from triplicate experiments. B) Confocal microscopy images of fibroblast cells on substrates after 24 h staining with Alexa-phalloidin: (left) cells on control tissue culture plates, (middle) nonconductive silk fibroin, and (right) conductive silk fibroin films. C) Electrochemically enhanced delivery of Texas-Red Gentamicin from conductive silk fibroin films in PBS (pH = 7.4) as determined by fluorescence spectroscopy. Cumulative release of Texas-Red Gentamicin from conductive silk fibroin films (expressed as a % of 1 μg): passive release (black bars) and electrically stimulated release (gray bars).

Electroactive materials are an emerging class of instructive biomaterials with a variety of biomedically relevant applications we see rich potential for in the foreseeable future.

Experimental Section

The full experimental details can be found in the Supporting Information.

Supporting Information

Supporting Information is available from the Wiley Online Library or from the author.

Acknowledgements

At Lancaster University, the authors thank Elisabeth Shaw of the Department of Biomedical and Life Sciences for access to a centrifuge, and Lorna Ashton of the Department of Chemistry for technical support with Raman spectroscopy. The authors thank Payame Noor University and the Iranian Ministry of Science for a Ph.D. studentship for S.T.M. The authors thank the Biotechnology and Biological Sciences Research Council (BBSRC) Networks in Industrial Biotechnology and Bioenergy (NIBB) "FoodWasteNet" (FWN, grant BB/L0137971/1) for a Proof of Concept Grant supporting G.R.H., and the LBNet NIBB for a Business Interaction Voucher (BB/L013738/1) supporting D.T. The authors thank the Engineering and Physical Sciences Research Council (EPSRC) for a Ph.D. studentship for M.D.A. (EP/R512564/1, 2065445). The authors thank the Ministry of Education in Saudi Arabia for a Ph.D. studentship for G.H.K.A. administered by the Saudi Arabian Cultural Bureau. The authors thank the British Council of Greece for the IELTS Award 2017 for V.K.O. The authors thank Lancaster University for a summer vacation scholarship for B.E.M. The authors thank the Royal Society for a Research Grant (RG160449) for J.G.H., a Newton International Fellowship (NF151479) for M.F., and an International Exchanges Grant (A103355) to support interactions between S.M., M.D.A., M.F.D., and J.G.H.

Conflict of Interest

The authors declare no conflict of interest.

Author Contributions

J.G.H. conceptualized the paper and prepared the original draft. Methodology, formal analysis, and investigation were carried out by all authors. S.T.M., G.R.H., V.K.O., and B.E.M. carried out materials preparation. D.T., G.H.K.A., G.R.A., N.R.H., and S.J.B. carried out materials characterization. S.M. performed cell culture. M.D.A., M.F., S.A.-Y., and B.E.M. were involved in drug delivery. B.J.R., M.F.D., and J.G.H. carried out data curation. All authors were involved in writing, reviewing, and editing. M.F., O.V.K., B.J.R., M.F.D., and J.G.H. did the supervision. J.G.H was involved in project administration. M.F., O.V.K., B.J.R., M.F.D., and J.G.H. were involved in funding acquisition.

Keywords

biomaterials, drug delivery, electrical stimulation, silk fibroin, stimuli-responsive materials

Received: February 27, 2020
Revised: April 22, 2020
Published online:

[1] W. W. Huang, S. J. Ling, C. M. Li, F. G. Omenetto, D. L. Kaplan, *Chem. Soc. Rev.* **2018**, *47*, 6486.
[2] J. G. Hardy, L. M. Romer, T. R. Scheibel, *Polymer* **2008**, *49*, 4309.
[3] S. C. Kundu, B. Kundu, S. Talukdar, S. Bano, S. Nayak, J. Kundu, B. B. Mandal, N. Bhardwaj, M. Botlagunta, B. C. Dash, C. Acharya, A. K. Ghosh, *Biopolymers* **2012**, *97*, 455.
[4] T. P. Nguyen, Q. V. Nguyen, V. H. Nguyen, T. H. Le, V. Q. N. Huynh, D. V. N. Vo, Q. T. Trinh, S. Y. Kim, Q. V. Le, *Polymers* **2019**, *11*, 1933.
[5] T. B. Aigner, E. DeSimone, T. Scheibel, *Adv. Mater.* **2018**, *30*, 1704636.
[6] M. Widhe, J. Johansson, M. Hedhammar, A. Rising, *Biopolymers* **2012**, *97*, 468.
[7] C. Holland, K. Numata, J. Rnjak-Kovacina, F. P. Seib, *Adv. Healthcare Mater.* **2019**, *8*, 1800465.
[8] T. D. Sutherland, J. H. Young, S. Weisman, C. Y. Hayashi, D. J. Merritt, *Annu. Rev. Entomol.* **2010**, *55*, 171.
[9] J. G. Hardy, T. R. Scheibel, *Prog. Polym. Sci.* **2010**, *35*, 1093.
[10] A. U. Ude, R. A. Eshkoor, R. Zulkifili, A. K. Ariffin, A. W. Dzuraidah, C. H. Azhari, *Mater. Des.* **2014**, *57*, 298.
[11] M. D. Ashton, J. G. Hardy, *Johnson Matthey Tech.* **2019**, *63*, 211.
[12] F. Khan, M. Tanaka, *Int. J. Mol. Sci.* **2017**, *19*, 17.
[13] P. S. Kowalski, C. Bhattacharya, S. Afewerki, R. Langer, *ACS Biomater. Sci. Eng.* **2018**, *4*, 3809.
[14] A. Leal-Egana, T. Scheibel, *Biotechnol. Appl. Biochem.* **2010**, *55*, 155.
[15] A. R. Murphy, D. L. Kaplan, *J. Mater. Chem.* **2009**, *19*, 6443.
[16] C. Vepari, D. L. Kaplan, *Prog. Polym. Sci.* **2007**, *32*, 991.
[17] A. M. Abdullah, X. L. Li, P. V. Braun, J. A. Rogers, K. J. Hsia, *Adv. Mater.* **2018**, *30*, 1801669.
[18] A. Balasubramanian, R. Morhard, C. J. Bettinger, *Adv. Funct. Mater.* **2013**, *23*, 4757.
[19] N. K. Guimard, N. Gomez, C. E. Schmidt, *Prog. Polym. Sci.* **2007**, *32*, 876.
[20] S. Naficy, G. M. Spinks, G. G. Wallace, *ACS Appl. Mater. Interfaces* **2014**, *6*, 4109.
[21] M. Nune, S. Manchineella, T. Govindaraju, K. S. Narayan, *Mater. Sci. Eng., C* **2019**, *94*, 17.
[22] V. Sencadas, C. Garvey, S. Mudie, J. J. K. Kirkensgaard, G. Gouadec, S. Hauser, *Nano Energy* **2019**, *66*, 104106.
[23] T. Srisawasdi, K. Petcharoen, A. Sirivat, A. M. Jamieson, *Mater. Sci. Eng., C* **2015**, *56*, 1.
[24] C. Y. Yan, Y. X. Ren, X. Y. Sun, L. M. Jin, X. L. Liu, H. L. Chen, K. J. Wang, M. Yu, Y. H. Zhao, *J. Photochem. Photobiol., B* **2020**, *202*, 111680.
[25] Y. Yang, X. L. Ding, T. Q. Zou, G. Peng, H. F. Liu, Y. B. Fan, *RSC Adv.* **2017**, *7*, 7954.
[26] M. Y. Zhang, B. L. Guo, *Macromol. Biosci.* **2017**, *17*, 1700147.
[27] Y. Ma, L. Chen, F. Y. Dai, Z. Li, *J. Biomater. Tissue Eng.* **2018**, *8*, 1629.
[28] N. Piri, V. Mottaghitalab, S. Arbab, *e-Polymers* **2013**, *13*, https://doi.org/10.1515/epoly-2013-0107.
[29] B. L. Guo, L. Glavas, A. C. Albertsson, *Prog. Polym. Sci.* **2013**, *38*, 1263.
[30] B. L. Guo, P. X. Ma, *Biomacromolecules* **2018**, *19*, 1764.
[31] T. Adali, E. Kavalci, I. Kurt, *J. Biotechnol.* **2014**, *185*, S36.
[32] S. Aznar-Cervantes, M. I. Roca, J. G. Martinez, L. Meseguer-Olmo, J. L. Cenis, J. M. Moraleda, T. F. Otero, *Bioelectrochemistry* **2012**, *85*, 36.
[33] D. L. Barreiro, Z. Martin-Moldes, J. J. Yeo, S. Shen, M. J. Hawker, F. J. Martin-Martinez, D. L. Kaplan, M. J. Buehler, *Adv. Mater.* **2019**, *31*, 1904720.
[34] S. Das, M. Sharma, D. Saharia, K. K. Sarma, E. M. Muir, U. Bora, *Biomed. Mater.* **2017**, *12*, 045025.
[35] J. G. Hardy, S. A. Geissler, D. Aguilar, M. K. Villancio-Wolter, D. J. Mouser, R. C. Sukhavasi, R. C. Cornelison, L. W. Tien, R. C. Preda, R. S. Hayden, J. K. Chow, L. Nguy, D. L. Kaplan, C. E. Schmidt, *Macromol. Biosci.* **2015**, *15*, 1490.
[36] J. G. Hardy, Z. Z. Khaing, S. J. Xin, L. W. Tien, C. E. Ghezzi, D. J. Mouser, R. C. Sukhavasi, R. C. Preda, E. S. Gil, D. L. Kaplan, C. E. Schmidt, *J. Biomater. Sci., Polym. Ed.* **2015**, *26*, 1327.
[37] Y. M. Niu, X. F. Chen, D. Y. Yao, G. Peng, H. F. Liu, Y. B. Fan, *J. Biomed. Mater. Res., Part A* **2018**, *106*, 2973.
[38] S. Y. Severt, S. Maxwell, J. Bontrager, J. M. Leger, A. R. Murphy, *J. Mater. Chem. B* **2017**, *5*, 8105.
[39] J. H. Tsui, N. A. Ostrovsky-Snider, D. M. P. Yama, J. D. Donohue, J. S. Choi, R. Chavanachat, J. D. Larson, A. R. Murphy, D. H. Kim, *J. Mater. Chem. B* **2018**, *6*, 7185.
[40] S. Tsukada, H. Nakashima, K. Torimitsu, *PLoS One* **2012**, *7*, e33689.

[41] C. Y. Wang, K. L. Xia, Y. Y. Zhang, D. L. Kaplan, *Acc. Chem. Res.* **2019**, *52*, 2916.
[42] Y. H. Zhao, C. M. Niu, J. Q. Shi, Y. Y. Wang, Y. M. Yang, H. B. Wang, *Neural Regener. Res.* **2018**, *13*, 1455.
[43] B. Tandon, A. Magaz, R. Balint, J. J. Blaker, S. H. Cartmell, *Adv. Drug Delivery Rev.* **2018**, *129*, 148.
[44] Z. L. Yue, S. E. Moulton, M. Cook, S. O'Leary, G. G. Wallace, *Adv. Drug Delivery Rev.* **2013**, *65*, 559.
[45] V. Pillay, T. S. Tsai, Y. E. Choonara, L. C. du Toit, P. Kumar, G. Modi, D. Naidoo, L. K. Tomar, C. Tyagi, V. M. K. Ndesendo, *J. Biomed. Mater. Res., Part A* **2014**, *102*, 2039.
[46] J. G. Hardy, D. J. Mouser, N. Arroyo-Curras, S. Geissler, J. K. Chow, L. Nguy, J. M. Kim, C. E. Schmidt, *J. Mater. Chem. B* **2014**, *2*, 6809.
[47] S. A. A. Shah, M. Firlak, S. R. Berrow, N. R. Halcovitch, S. J. Baldock, B. M. Yousafzai, R. M. Hathout, J. G. Hardy, *Materials* **2018**, *11*, 1123.
[48] R. Nazarov, H. J. Jin, D. L. Kaplan, *Biomacromolecules* **2004**, *5*, 718.
[49] X. Hu, D. Kaplan, P. Cebe, *Thermochim. Acta* **2007**, *461*, 137.
[50] I. Uguz, M. Ganji, A. Hama, A. Tanaka, S. Inal, A. Youssef, R. M. Owens, P. P. Quilichini, A. Ghestem, C. Bernard, S. A. Dayeh, G. G. Malliaras, *Adv. Healthcare Mater.* **2016**, *5*, 3094.
[51] X. Hu, D. Kaplan, P. Cebe, *Macromolecules* **2006**, *39*, 6161.
[52] D. N. Rockwood, R. C. Preda, T. Yucel, X. Q. Wang, M. L. Lovett, D. L. Kaplan, *Nat. Protoc.* **2011**, *6*, 1612.
[53] P. Monti, G. Freddi, A. Bertoluzza, N. Kasai, M. Tsukada, *J. Raman Spectrosc.* **1998**, *29*, 297.
[54] P. Monti, G. Freddi, A. Bertoluzza, N. Kasai, S. Tsukada, *J. Raman Spectrosc.* **1998**, *29*, 297.
[55] P. Monti, G. Freddi, M. Tsukada, A. Bertoluzza, T. Asakura, *Spectrosc. Biol. Mol.: New Dir.* **1999**, 81.
[56] P. Monti, P. Taddei, G. Freddi, T. Asakura, M. Tsukada, *J. Raman Spectrosc.* **2001**, *32*, 103.
[57] P. Monti, P. Taddei, G. Freddi, T. Asakura, M. Tsukada, *J. Raman Spectrosc.* **2001**, *32*, 103.
[58] M. Šetka, R. Calavia, L. Vojkůvka, E. Llobet, J. Drbohlavová, S. Vallejos, *Sci. Rep.* **2019**, *9*, 8465.
[59] M. Trchová, Z. Morávková, M. Bláha, J. Stejska, *Electrochim. Acta* **2014**, *122*, 28.
[60] T. Asakura, K. Isobe, S. Kametani, O. T. Ukpebor, M. C. Silverstein, G. S. Boutis, *Acta Biomater.* **2017**, *50*, 322.
[61] X. G. Li, Z. Z. Hou, M. R. Huang, M. G. Moloney, *J. Phys. Chem. C* **2009**, *113*, 2586.
[62] Y. Liu, D. A. Peterson, H. Kimura, D. Schubert, *J. Neurochem.* **1997**, *69*, 581.
[63] F. Robotti, S. Bottan, F. Fraschetti, A. Mallone, G. Pellegrini, N. Lindenblatt, C. Starck, V. Falk, D. Poulikakos, A. Ferrari, *Sci. Rep.* **2018**, *8*, 8465.
[64] M. Ventre, C. F. Natale, C. Rianna, P. A. Netti, *J. R. Soc., Interface* **2014**, *11*, 20140687.
[65] G. G. Malliaras, *Biochim. Biophys. Acta, Gen. Subj.* **2013**, *1830*, 4286.
[66] R. Vadlapatla, E. Y. Wong, S. G. Gayakvvad, *J. Drug Delivery Sci. Technol.* **2017**, *41*, 359.
[67] M. Humenik, A. M. Smith, T. Scheibel, *Polymers* **2011**, *3*, 640.
[68] O. Tokareva, V. A. Michalczechen-Lacerda, E. L. Rech, D. L. Kaplan, *Microb. Biotechnol.* **2013**, *6*, 651.
[69] H. M. Herold, T. Scheibel, *Z. Naturforsch., C* **2017**, *72*, 365.
[70] J. G. Hardy, T. R. Scheibel, *Biochem. Soc. Trans.* **2009**, *37*, 677.